ISSN 0030-400X, Optics and Spectroscopy, 2017, Vol. 122, No. 5, pp. 816–825. © Pleiades Publishing, Ltd., 2017.
Original Russian Text © E.V. Aksenova, A.A. Karetnikov, A.P. Kovshik, E.S. Krainyukov, A.V. Svanidze, 2017, published in Optika i Spektroskopiya, 2017, Vol. 122, No. 5, pp. 844–854.

PHYSICAL OPTICS

The Influence of an External Electric Field on the Propagation of Light Waves in Cholesteric Liquid Crystal Cells

E. V. Aksenova*, A. A. Karetnikov, A. P. Kovshik***, E. S. Krainyukov****, and A. V. Svanidze*******

St. Petersburg State University, St. Petersburg, 199034 Russia

**e-mail: e.aksenova@spbu.ru*

***e-mail: akaret@mail.ru*

****e-mail: SashaKovshik@yandex.ru*

*****e-mail: bacoom888@gmail.com*

******e-mail: svanastation@mail.ru*

Received December 6, 2016

Abstract—The specific features of light transmission in a cholesteric liquid crystal (LC) cell with a director rotated by 90° have been investigated. In this structure, where a light wave is incident at a large angle with respect to the LC surface, the light is reflected (refracted) in the LC layer near the opposite boundary. It is shown that the application of an electric field changes the character of extraordinary wave refraction, as a result of which light starts passing through a cell. The transmission threshold voltage is determined, and its dependence on the angle of incidence of light is obtained. The dependence of the transmitted-light intensity on the voltage across the cell is obtained as well. The same dependences are also derived by numerical calculations with allowance for the turning points and extinction.

DOI: 10.1134/S0030400X17050022

INTRODUCTION

Since liquid crystals (LCs) are widely used in practice, researchers pay much attention to their optical properties and behavior in external fields. The issue is that the optical properties of thin LC layers can easily be controlled using an electric field: an external electric field causes reorientation of the LC director, due to which one can control the intensity of light passing through the LC layer.

The unique electro-optical properties of LCs are used in displays, data-transfer systems, and various optical devices [1–4]. LCs serve as a basis for electro-optical modulators, indicators operating in different temperature ranges, and biosensors [5], as well as media for recording holographic gratings and dynamic holograms [6, 7].

LC cells are rather complex systems. To describe the LC behavior, one must know a number of parameters: Frank moduli, permittivity, and the LC–substrate anchoring energy. Setting the orientation of LC molecules on the cell boundaries affects the director distribution in the cell volume, thus influencing the optical characteristics of the cell.

It is rather difficult to describe the behavior of LC systems in external fields for the following reason: the director distribution and, therefore, the optical characteristics change throughout the LC sample thickness. In addition, the presence of optical anisotropy calls for the tensor description of the problem. Calculating the intensities of light beams passing through these systems and analyzing their trajectories, one can investigate the changes in the LC local structure as a function of the applied external field.

The description of the LC structure in external fields is a difficult problem, especially in the case of strong fields (exceeding the Freedericksz threshold). The presence of spatial helicoidal structure complicates the mathematical description of the Freedericksz transition in external fields. The Freedericksz transition in cholesteric LCs (CLCs) was considered for the first time by Leslie [8]. Note that, in contrast to nematics in chiral systems, there is a significant difference between the descriptions of the Freedericksz effect in electric and magnetic fields. The reason for this is that the electric field in cholesterics is inhomogeneous. This problem was considered in detail in [9–12].

The problem of propagation of light incident at a certain angle on an anisotropic medium with arbitrarily directed optical axes has been solved theoretically using different methods. In particular, numerical methods have been used to a very great extent [13–17]. Much attention is also paid to exact and approximate

analytical methods [18–21], the mode-coupling method [22, 23], and methods of geometrical optics [24, 25].

In this study, we consider a cell with a helix pitch greatly exceeding the light wavelength. The so-called "Mauguin adiabatic approximation" is used to describe the wave propagation in such systems [26]. The properties of these media change gradually on the scale of λ, due to which one can use methods of the Wentzel–Kramers–Brillouin (WKB) type. The problem of propagation of electromagnetic waves in locally isotropic media with smooth inhomogeneities was solved in [27, 28]. The corresponding problem for CLCs with a large pitch in the case of oblique incidence of light was solved in [29]. Here, light also propagates in the adiabatic mode: there are two normal waves, locally ordinary and locally extraordinary, the polarization vectors of which are determined by the local directions of the optical axis and wave vector at a given point. Under these conditions, the wave-vector component transverse to the spiral axis is retained, and its length (the wave number) is determined from the local dispersion equation [29].

When an extraordinary ray is incident on a CLC at an angle exceeding some minimum value, the extraordinary ray is rotated (reflected) in the medium and emerges from it [30]. Note that the rotation occurs inside the sample rather than on its surface.

When a light beam propagates in a fluctuating medium, it loses energy upon scattering. This loss is described by the extinction coefficient. The latter coincides with the total scattering cross section (the scattered radiation intensity integrated over all scattering angles and normalized to unit volume and unit incident-wave intensity). A homogeneous uniaxial medium is characterized by two extinction coefficients, which are related to the scattering of ordinary and extraordinary waves [31, 32]. Since the ray path length in the cells under consideration may be rather large, we will need to take into account the damping caused by the extinction when calculating the transmitted-light intensity.

In this paper, we report the results of an experimental and theoretical study of the propagation of light in CLCs in an external electric field exceeding the Freedericksz threshold. The distortion of the LC structure and the corresponding specific features of the extraordinary-ray propagation were analyzed. The internal refraction of a ray in a cholesteric due to the spatial change in the optical axis direction in the medium was investigated. The propagation of light was theoretically described within the geometrical optics approximation, where the ratio of the LC helix pitch to the light wavelength was used as a large parameter. Theoretical and experimental dependences of the minimum transmission voltage on the limiting angle of refraction and the transmitted-light intensity on the voltage at a fixed angle of incidence were obtained. Despite the fact that we considered a CLC cell with a director rotation by 90°, the method used is also suitable for other LC cell geometries. The analysis of different cell geometries and comparison of their characteristics is of great interest for determining optimal cell properties in various applications.

The paper is organized as follows. Section 1 contains the equations based on which one can find the director distribution in an external electric field. In Section 2, the propagation of electromagnetic waves in a uniaxial medium is briefly described and a solution of the wave equation by the WKB method in the first order relative to the large parameter is presented. In Section 3, the light-intensity losses related to scattering are considered. The experimental setup is described in Section 4. In Section 5, the experimental data are compared with the results of numerical calculations.

1. FREE ENERGY AND DIRECTOR DISTRIBUTION IN THE CELL VOLUME

The system under consideration consists of two plane-parallel glass plates with deposited thin transparent conducting layers, between which a CLC layer is placed. The LC is oriented in a certain way: the helix axis is perpendicular to the plate planes. A voltage can be applied to the plates so that the electric field strength $\mathbf{E}$ between the plates is parallel to the CLC helix axis. The free energy of this system is described using the director unit vector $\mathbf{n}(\mathbf{r})$ (which indicates the preferred molecular orientation at a given point) as follows:

$$F_{\text{tot}} = F_e + F_f + F_{sf}. \tag{1}$$

The first term is the free Frank energy; it describes the LC strain energy in the bulk:

$$F_e = \frac{1}{2}\int [K_{11}(\text{div}\mathbf{n})^2 + K_{22}(\mathbf{n}\text{curl}\mathbf{n} + q_0)^2 + K_{33}(\mathbf{n}\times\text{curl}\mathbf{n})^2]dV, \tag{2}$$

where K_{11}, K_{22}, K_{33} are the Frank moduli; $p_0 = 2\pi/q_0$ is the helix pitch; and V is the volume occupied by the CLC.

The last term (F_{sf}) is the LC–substrate surface anchoring energy. Hereinafter, the LC anchoring with the surface is considered rigid: $F_{sf} \gg F_e + F_f$. It will be taken into account by imposing the boundary conditions on the director:

$$\mathbf{n}(0) = \mathbf{n}^{0(1)}, \quad \mathbf{n}(L) = \mathbf{n}^{0(2)}, \tag{3}$$

where vectors $\mathbf{n}^{0(1)}$ and $\mathbf{n}^{0(2)}$ describe the easy orientation axes on the lower and upper faces of the cell, respectively.

To describe the optical properties of an LC cell, one must know the director vector distribution in the cell bulk. The distribution $\mathbf{n}(\mathbf{r})$ can be obtained by direct minimization of the free energy using the method proposed in [21]. Below, we report only the main equations of this method and the conclusions drawn from its use.

Let us introduce a Cartesian coordinate system, where the z axis is directed perpendicular to the substrate planes, the xOy plane coincides with the substrate plane, and the x axis is directed arbitrarily. We assume that the arrangement of the substrate planes corresponds to the planes $z = 0$ and $z = L$. In the absence of an external field in the equilibrium state, the director vector is perpendicular to the z axis at each point. The system is assumed to be homogeneous in each plane $z = \text{const}$, which means that $\mathbf{n}(\mathbf{r}) = \mathbf{n}(z)$. Then, in the spherical coordinates, $\mathbf{n}(z) = (\sin\theta(z)\cos\phi(z), \sin\theta(z)\sin\phi(z), \cos\theta(z))$, where angles θ and ϕ are counted from the z and x axes, respectively.

In this case, the contributions to the free energy of the system can be transformed as follows. The first term in Eq. (1) takes the form

$$F_e = \frac{V}{2}K_{22}q_0^2 + \frac{S_\perp}{2}\int_0^L [A(\theta)(\theta')^2 + B(\theta)(\phi')^2 - 2C(\theta)\phi']dz, \quad (4)$$

where $S_\perp$ is the substrate area, $V = LS_\perp$,

$$A(\theta) = K_{11}\sin^2\theta + K_{33}\cos^2\theta, \quad (5)$$

$$B(\theta) = \sin^2\theta(K_{22}\sin^2\theta + K_{33}\cos^2\theta), \quad (6)$$

$$C(\theta) = q_0K_{22}\sin^2\theta. \quad (7)$$

It is convenient to write the contribution of the external field to the energy in terms of voltage U applied to the plates:

$$F_f = -\frac{S_\perp U^2}{8\pi\int_0^L(\tilde{\varepsilon}_\perp + \tilde{\varepsilon}_a\cos^2\theta)^{-1}dz}, \quad (8)$$

where $\tilde{\varepsilon}_{\alpha\beta} = \tilde{\varepsilon}_\perp\delta_{\alpha\beta} + \tilde{\varepsilon}_a n_\alpha n_\beta$ is the permittivity tensor of the medium; $\tilde{\varepsilon}_a = \tilde{\varepsilon}_\parallel - \tilde{\varepsilon}_\perp$ is the permittivity anisotropy; $\tilde{\varepsilon}_\perp$ and $\tilde{\varepsilon}_\parallel$ are the permittivities in the directions along and perpendicular to the director, respectively; and $\delta_{\alpha\beta}$ is the Kronecker delta ($\alpha, \beta = x, y, z$). The permittivity values are taken at the frequency of the applied electric field.

Let us divide the sample into N layers in the direction of the Oz axis. We assume that the orientation of the director vector in each layer is homogeneous and set by angles θ and ϕ. Then we will construct a set of values $\theta_i = \theta(z_i)$, $\phi_i = \phi(z_i)$, $z_i = iL/N$, $i = 0, 1, ..., N$, which determine the director distribution in the cell bulk. Using the finite-element method, one can express the total free energy in terms of θ_i and ϕ_i. Having minimized the free energy over them, we obtain the director configurations at different values of an external electric field.

2. PROPAGATION OF LIGHT IN LC CELLS: GEOMETRICAL-OPTICS APPROXIMATION

In this section, we consider the propagation of light in CLC cells. Note that permittivity tensor $\hat{\varepsilon}$, which determines the optical properties of the medium, is taken at the optical frequency of measurements. Below, we assume the medium to be nonmagnetic; i.e., permeability tensor $\mu_{\alpha\beta} = \delta_{\alpha\beta}$. We are interested in solutions to the wave equation. Let us consider the case where a wave is incident on the plane $z = 0$. We assume that our system is characterized by a large parameter: the ratio of the helix pitch to the light wavelength, $\Omega = p_0/\lambda$. Therefore, the wave equation will be solved using the WKB method [33]. Within the framework of this method, we restrict ourselves to the first two orders with respect to large parameter Ω. The light-wave field can then be written [34] in the form

$$\mathbf{E}_\pm^{(j)}(\mathbf{r}) = A_\pm^{(j)}(\mathbf{k}_\perp; z, z_0)\mathbf{e}_\pm^{(j)}(\mathbf{k}_\perp, z) \times \exp\left(i\mathbf{k}_\perp\mathbf{r}_\perp + i\int_{z_0}^z k_{z\pm}^{(j)}(\mathbf{k}_\perp, z')dz'\right), \quad (9)$$

where (j) is the wave type (ordinary (o) or extraordinary (e)), $A_\pm^{(j)}$ are the wave amplitudes, $z_0 = 0$, $\mathbf{e}_\pm^{(j)}$ are the polarization vectors, $\mathbf{k} = (\mathbf{k}_\perp, k_z)$ is the wave vector, and $\mathbf{k}_\perp$ is a two-dimensional vector (it is independent of coordinates, and its magnitude is determined by the angle of incidence of light on the medium). The longitudinal component of the wave vector, k_z, which has a rather complicated form, can be derived [34] from the eikonal equation

$$k_{z\pm}^{(o)} = \pm\sqrt{k_0^2\varepsilon_\perp - k_\perp^2}, \quad (10)$$

$$k_{z\pm}^{(e)} = \frac{k_0}{\varepsilon_\perp + \varepsilon_a\cos^2\theta} \times\left(-\frac{k_\perp}{k_0}\varepsilon_a\sin\theta\cos\theta\cos\phi \pm \varepsilon_\perp\sqrt{D(k_\perp, \theta, \phi)}\right), \quad (11)$$

where

$$D(k_\perp, \theta, \phi) = \varepsilon_\parallel\left(1 - \frac{k_\perp^2}{k_0^2\varepsilon_\perp} + \frac{\varepsilon_a}{\varepsilon_\perp}\cos^2\theta\right) + \frac{k_\perp^2\varepsilon_a}{k_0^2\varepsilon_\perp}\sin^2\theta\sin^2\phi, \quad (12)$$

$k_0 = 2\pi/\lambda$. Expression (9) describes four possible solutions to the wave equation.

In the system under consideration, the refractive index of the medium may decrease along the extraordinary-ray propagation path. In this case, the ray may undergo total internal reflection (i.e., the wave vector gradually changes its direction to opposite during propagation). At some point of the medium ($z = z^*$), the function $D(\mathbf{k}_\perp, \theta(z^*), \phi(z^*)) = 0$, after which it becomes negative. This means that $k_z^{(e)}$ acquires an imaginary additive and the wave begins to exponentially decay. In reality, the wave undergoes total reflection at this point. The wave, being reflected from some layer in the medium, starts propagating in the backward direction with respect to the z axis. The points at which $D(\mathbf{k}_\perp, \theta(z^*), \phi(z^*)) = 0$ are referred to as "turning points" in the theory of differential equations. It is a rather difficult problem to construct the field in the vicinity of these points, because the WKB method does not work there. Since we are interested in the light transmission through the cell, the presence and location of turning points is of key importance.

3. EFFECT OF EXTINCTION

When the angle of incidence of light is sufficiently large, the extraordinary-ray propagation path in a CLC cell is fairly long. As a result, the intensity of the light beam transmitted through the cell decreases (because of light scattering). This intensity loss is described by extinction coefficient σ:

$$I(L) = I(0)\exp\left(-\int_0^L \sigma(l)dl\right), \quad (13)$$

where $I(0)$ is the incident-light intensity and dl is an element of the ray-path length. The expression for the extinction in CLC is given in the Appendix.

The element of the ray-path length can written as

$$dl = dz\sqrt{1 + \left(\frac{d\mathbf{r}_\perp}{dz}\right)^2}. \quad (14)$$

The tangent at each point of the ray path is parallel to the Poynting vector $\mathbf{S}$:

$$\frac{d\mathbf{r}_\perp(z)}{dz} = \frac{\mathbf{S}_\perp(z)}{S_z(z)}. \quad (15)$$

The CLC under consideration is a locally uniaxial medium. For these media, the directions of the Poynting and wave vectors are related as follows: $\mathbf{S} \parallel \hat{\varepsilon}\mathbf{k}$. Then we have

$$\frac{\mathbf{S}_\perp(z)}{S_z(z)} = \frac{(\hat{\varepsilon}(z)\mathbf{k}^{(e)}(z))_\perp}{(\hat{\varepsilon}(z)\mathbf{k}^{(e)}(z))_z}, \quad (16)$$

$$\frac{d\mathbf{r}_\perp(z)}{dz} = \frac{\mathbf{n}(z)k_\perp \cos\phi(z)\varepsilon_a + \mathbf{k}_\perp\varepsilon_\perp}{k_z^{(e)}\varepsilon_\perp}. \quad (17)$$

Expressions (14) and (17) and the expression for the extinction coefficient derived in Appendix make it possible to calculate the light-scattering loss (13).

4. EXPERIMENTAL

The experimental cell for studying the refraction in CLC consisted of two glass trapezoidal prisms, PR1 and PR2, with 50 × 25 mm bases and a height of 18 mm (Fig. 1). The tilt angle made by the lateral faces with the bases was 68°. Glass refractive index n_g was 1.712 for a wavelength of $\lambda = 632.8$ nm. Transparent conducting coatings (electrodes) and thin polyimide layers were deposited on the prism bases. The polyimide layers were rubbed to form a planar LC orientation, which provides rigid anchoring between the LC and the prism surface. In this case, the LC director on the boundary layer (on which light falls) is directed perpendicular to the drawing plane (Fig. 1). On the second layer boundary, the director lies in the drawing plane. The necessary LC-layer thickness (8 μm) was set using Teflon spacers. The gap between the prisms was filled with a CLC mixture having a helix pitch of 32 μm. The mixture consisted of LC-1466 (NIOPIK) and VICh-3 active additive (Vilnius University, Lithuania). The Frank moduli for LC-1466 are $K_{11} = 1.1 \times 10^{-6}$ dyn, $K_{22} = 0.38 \times 10^{-6}$ dyn, and $K_{33} = 0.99K_{11}$. Dielectric anisotropy $\tilde{\varepsilon}_a$ of LC-1466 in the frequency range from 500 Hz to 10 kHz is 12.3, and the permittivity in the direction across the director is $\tilde{\varepsilon}_\perp = 6.95$. The principal values of the permittivity tensor, $\varepsilon_\parallel$ and $\varepsilon_\perp$, for wavelength $\lambda = 632.8$ nm are 2.86 and 2.28, respectively. At specified values of the layer thickness and helix pitch, the director rotated by 90° when passing from one layer boundary to the other.

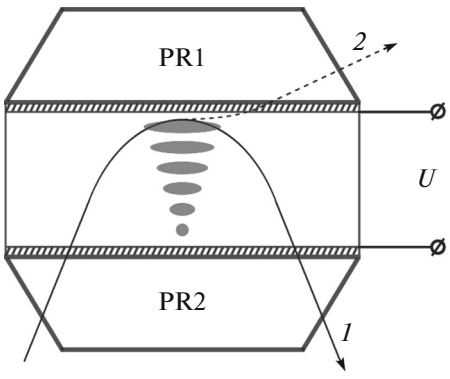

Fig. 1. A liquid crystal cell consisting of two trapezoidal glass prisms PR1 and PR2, with thin polyimide layers and transparent conducting coatings deposited on their bases. The director is oriented perpendicular to the drawing plane on the lower face of the LC cell and lies in the drawing plane on the upper face. (*1*) Schematic path of extraordinary ray in the absence of an electric field. (*2*) The extraordinary ray starts passing through the cell at some voltage *U*.

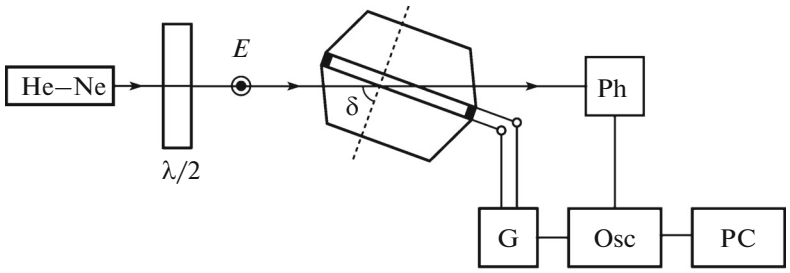

Fig. 2. Schematic of the experimental setup: (He–Ne) helium–neon laser, (λ/2) half-wave plate, (Ph) photodetector, (G) generator, (Osc) oscilloscope, and (PC) computer.

A block diagram of the experimental setup is presented in Fig. 2 (top view). A helium–neon laser beam with wavelength $\lambda = 632.8$ nm and diameter of 1 mm was directed on the LC cell under study through half-wave plate $\lambda/2$. The half-wave plate was used to orient the incident-ray polarization vector parallel to the LC director at the glass–LC interface. The light then arrived at photodetector Ph, the signal from which was recorded by digital oscilloscope Osc (ASK-3106) and a computer. A control ac rectangular voltage from an Aktakom ANR-3122 generator was applied (through a commutator) to the cell electrodes and the oscilloscope. The commutator generated pulses with a duration from 0.1 to 5 s. To change the angle of incidence of the light beam on the LC layer, the cell was installed on a rotating table equipped with an angle reading device (reading accuracy 1 min).

Threshold voltage U_{th} of light transmission through the cell was determined using the dependence of transmitted-light intensity I on applied voltage U. The threshold voltage was considered to be the voltage at which the transmitted-light intensity became no less than 10% of the incident-light intensity. The experimental data are shown in Figs. 4 and 5 (next section) in comparison with the results of numerical calculations.

5. CALCULATION RESULTS

Let us first consider the penetration depth of an extraordinary ray into an LC layer in the absence of an external electric field. In this case, the expression for the penetration depth can be obtained analytically. We introduce a Cartesian coordinate system so as to satisfy the equality $\mathbf{k} = (k_\perp, 0, k_z(z))$. In turn, the director takes the form $\mathbf{n} = (\cos(q_0 z + \phi_0), \sin(q_0 z + \phi_0), 0)$, where $\phi_0 = \pi/2$ and $q_0 L = \phi_{\text{tot}}$. Angle ψ between the wave vector and director is then given by the relation

$$\cos\psi = \frac{k_\perp \cos(q_0 z + \phi_0)}{|\mathbf{k}|}. \quad (18)$$

At turning point z_* the wave-vector component k_z is zero. Snell's law for an extraordinary ray at point z_* is $n^{(e)}(z_*) = n_g \sin\delta$, where δ is the angle of incidence of light on the lower boundary of the LC cell and n_g is the refractive index of glass. Using the latter, one can easily obtain a relation for the penetration depth:

$$\cos(2q_0 z_* + 2\phi_0) = \frac{2\varepsilon_\perp\varepsilon_\parallel - (\varepsilon_\perp + \varepsilon_\parallel)n_g^2 \sin^2\delta}{\varepsilon_a n_g^2 \sin^2\delta}. \quad (19)$$

For the cell under consideration, we have

$$z_* = L - \frac{L}{\pi}\arccos\left(\frac{2\varepsilon_\perp\varepsilon_\parallel - (\varepsilon_\perp + \varepsilon_\parallel)n_g^2 \sin^2\delta}{\varepsilon_a n_g^2 \sin^2\delta}\right). \quad (20)$$

When an external electric field is switched on, wave-vector component k_z is nonzero at the turning point. In this case, dependence $z_*(\delta)$ can be obtained numerically. Minimizing the free energy at a certain electric voltage, we obtain the director distribution in the cell volume, i.e., sets of values $\theta(z_i)$ and $\phi(z_i)$ $(i = 0,1, \ldots, N)$ for a given U value. Substituting them into function $D(k_\perp, \theta(z), \phi(z))$, one can easily find the layer $z_i^* < z < z_{i+1}^*$ in which it changes sign. The turning point is located specifically in this layer. The coordinate of the midplane of this layer is taken to be the ray penetration depth in the cell. Figure 3 shows the dependence of the penetration depth on the angle of incidence of light on the LC at different voltages. One can see that the penetration depth decreases with an increase in the angle of incidence, and, at a fixed angle of incidence, increases with an increase in voltage. At large angles of incidence, the penetration depth depends weakly on voltage.

We experimentally obtained the dependence of the minimum transmission voltage on the limiting angle of refraction for the cell under consideration, i.e., the dependence on the largest angle of incidence of light on the glass–LC interface at which light still passes through the cell. Below we report a calculation of this dependence.

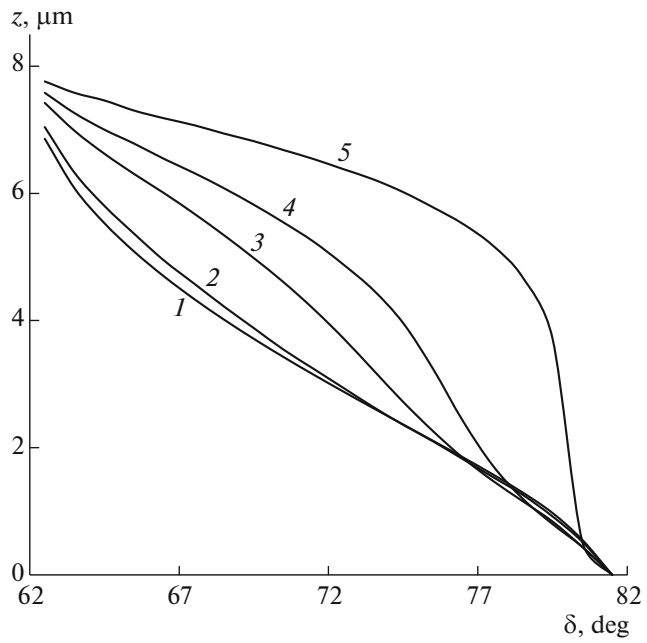

Fig. 3. Dependences of the extraordinary-ray penetration depth on the angle of incidence of light on the LC layer at different voltages: U = (*1*) 0, (*2*) 1.2, (*3*) 1.35, (*4*) 1.5, and (*5*) 2 V.

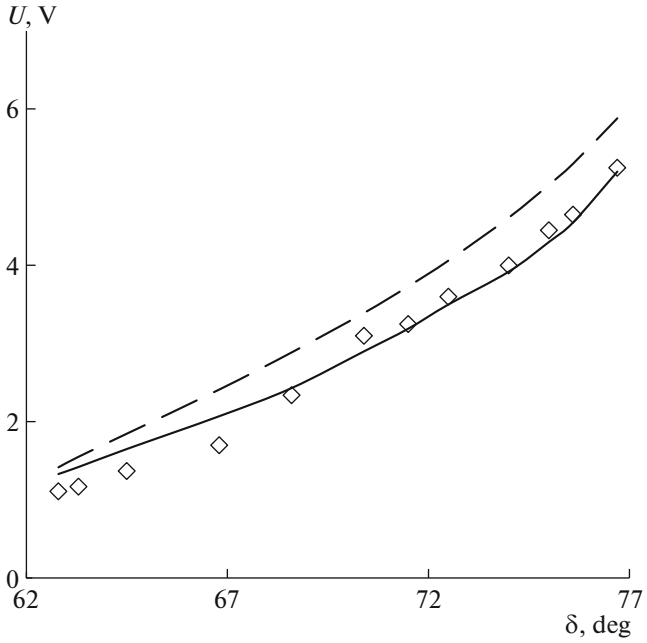

Fig. 4. Dependence of the minimum transmission voltage on the angle of incidence of light on the LC layer: (◊) experimental data, (dashed line) the result of the numerical calculation on the assumption that the percolation occurs at a distance equal to the light wavelength, and (solid line) the result of the numerical calculation on the assumption that the percolation occurs at a distance larger than the light wavelength by a factor of 1.2.

The position of the turning point depends on $k_\perp = k_0 n_g \sin\delta$. The range of δ values at which turning points exist is determined by the condition

$$\frac{\sqrt{\varepsilon_\perp}}{n_g} \le \sin\delta \le \frac{\sqrt{\varepsilon_\parallel}}{n_g}. \qquad (21)$$

Having chosen an appropriate δ value, one can make the ray rotate at a rather small distance from the upper boundary of the cell. For the angular range given by (21), the director orientation on the upper boundary for the cell geometry under consideration provides extraordinary-ray rotation in the cell bulk. Strictly speaking, the geometric optics is inapplicable in the vicinity of turning point, where the optical properties of the medium significantly change at distances on the order of the light wavelength. Modes may be transformed near these points. A possible consequence of this transformation is, e.g., percolation. This effect becomes pronounced if the turning point is located at a distance of $\le\lambda$ from the upper cell boundary. In this case, the transmitted-light intensity differs from zero due to the percolation. At the same time, if the turning point is located at a distance larger than λ from the upper boundary, the percolation barely manifests itself. Thus, if the turning point lies at a distance of $\propto\lambda$ from the upper cell boundary at fixed U and δ values, we assume that this voltage and angle correspond to the minimum transmission voltage for a given angle of incidence at which a wave does not pass through the cell. At higher voltages or smaller angles the wave passes through the cell.

The dependence of the minimum transmission voltage on the limiting angle of refraction was calculated as follows. First, the director distribution in the cell volume (i.e., sets of $\theta(z_i)$ and $\phi(z_i)$ values ($i = 0, 1, \ldots, N$)) was found for a fixed U by minimizing the free energy (1). The thus-found values were substituted into expression (12), as well as the angles of incidence δ from the range specified by (21). The δ value at which the turning point is located at a distance of $\propto\lambda$ from the upper cell boundary was determined from the set of equations for turning points: $D(\mathbf{k}_\perp, \theta(z_i), \phi(z_i)) = 0$. Specifically this δ value is the limiting angle of refraction.

Figure 4 shows the dependences of the minimum transmission voltage on the angle of incidence, both experimental and obtained by numerical calculation. The dashed line corresponds to the turning-point location at a distance equal to the light wavelength from the upper cell boundary. The best coincidence with the experimental data was observed for the calculation with the turning point located at a distance of 1.2λ from the upper boundary. The results of this calculation are shown in Fig. 4 by a solid line. One can see that the minimum transmission voltage increases with an increase in the angle of incidence. This behavior

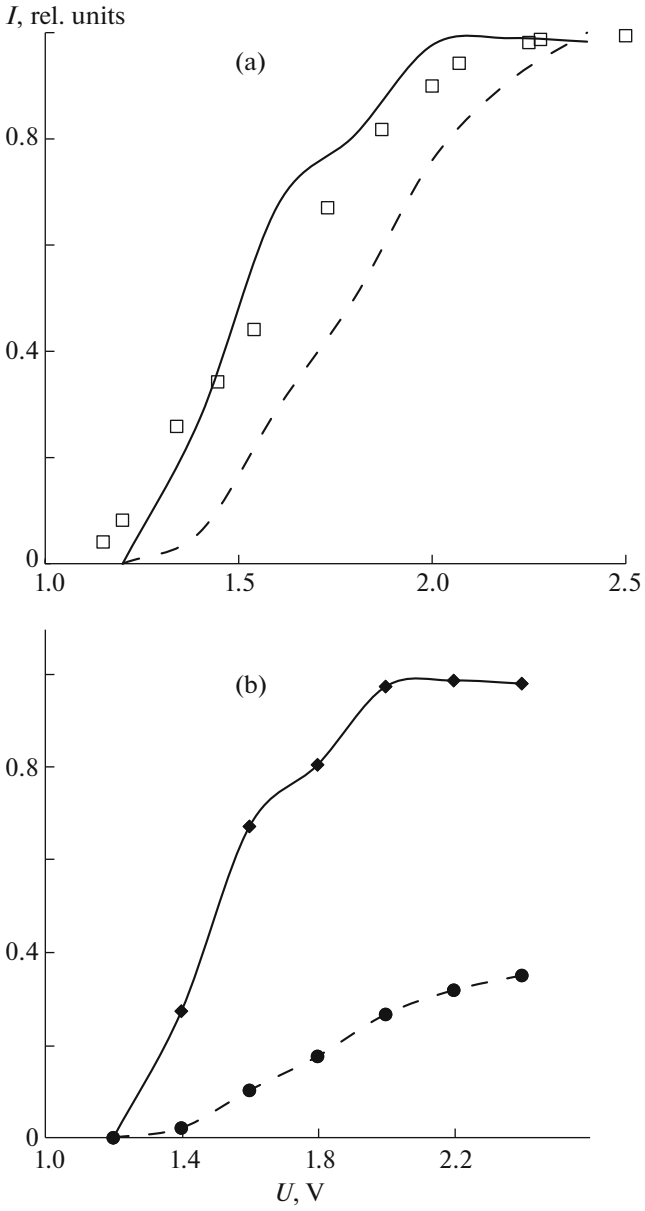

Fig. 5. Dependence of the transmitted-light intensity for an extraordinary ray on the voltage applied to the cell (the angle of incidence is $\delta = 63°$). (a) The intensity is normalized to the maximum transmission intensity: (squares) experimental data, (solid line) damping coefficient A is disregarded, and (dashed line) damping coefficient is taken into account. (b) The intensity is normalized to the incident-light intensity: (symbols) results of numerical calculation, (solid line) damping coefficient A is disregarded, and (dashed line) damping coefficient is taken into account.

can be explained as follows: at large angles of incidence the penetration depth becomes small, and, as can be seen in the previous figure, a higher voltage must be applied to make a ray start passing through the cell. A similar behavior of the dependence was observed for an LC cell with a director rotation by 180°, which was studied in [34].

The existence of turning points affects the light intensity transmitted through the cell. If turning points are absent, the transmitted-light intensity can be found using the expression

$$I(L) = I(0)\exp\left(-\int_0^L \sigma(z)\sqrt{1+\left(\frac{d\mathbf{r}_\perp}{dz}\right)^2}dz\right), \qquad (22)$$

where the expression for $\sigma(z)$ is given in Appendix (A.20). The dependence of extinction on z manifests itself in the following way: the angle between the director and wave vector changes while a wave penetrates into the LC bulk along the Oz axis. Integral (22) can be calculated from the Simpson formula using the sets θ_i and ϕ_i ($i = 0,1, \ldots, N$) obtained by minimizing energy (1). These sets are substituted into the expression for extinction (A.20) and the tangent at each point of the ray path (17). In the presence of turning points located at a distance from the upper cell boundary that is smaller than the light wavelength, the integration in expression (22) for intensity must be performed up to the turning point $z = z_*$:

$$I_* = I(0)\exp\left(-\int_0^{z_*} \sigma(z)\sqrt{1+\left(\frac{d\mathbf{r}_\perp}{dz}\right)^2}dz\right). \qquad (23)$$

One can also estimate the damping coefficient, which is related to the occurrence of the imaginary part in the z component of the wave vector at $z > z_*$:

$$A = \exp\left(-2\int_{z_*}^{L} \mathrm{Im}k_z(z)dz\right). \qquad (24)$$

The experimental and numerically calculated dependences of the transmitted-light intensity on voltage at a fixed angle of incidence are shown in Fig. 5a. The transmitted-light intensity linearly increases with an increase in voltage from 1.1 to 2 V. The intensities are normalized to the maximum transmission intensity. One can see that the experimental data and the results of numerical calculations are in good agreement. For comparison, Fig. 5b shows also the results of numerical calculations normalized to the incident-light intensity. The numerical calculations also yield a linear increase in intensity (Fig. 5b, solid line). The consideration of the damping coefficient for this system reduces the transmitted-light intensity by more than a half.

CONCLUSIONS

We obtained the director distributions in the LC cell volume at different voltages using a method based on the direct minimization of free energy [21]. With

the director distribution known, the dependences of the extraordinary-ray penetration depth on the angle of incidence at different voltages were numerically constructed. In the experiment, the angle of incidence is set with an error of 0.1°, due to which the depth of light penetration into the LC layer can be gradually changed. Thus, one has a unique possibility of studying the local orientational structure of the LC director and the dynamics of its change in external electric fields. Note that the light propagation was theoretically described within the framework of the geometrical optics approximation, where the ratio of the LC helix pitch to the light wavelength was used as a large parameter. Both theoretical and experimental dependences of the minimum transmission voltage on the limiting angle of refraction and the transmitted-light intensity on voltage at a fixed angle of incidence were determined. The calculations were carried out without any simplifying assumptions about the LC properties. All Frank moduli, the permittivity anisotropy, and the electric field inhomogeneity in the LC were taken into account. The theoretical description also took into account the presence of turning points for an extraordinary ray in the sample. The single adjustable parameter in the calculations was the depth at which light percolation occurs. Changing this depth, one can obtain good agreement between the experimental data and the results of numerical calculation. Note that the director distribution is confirmed only indirectly, because the transmitted-light intensity is an integral characteristic, whereas the minimum transmission voltage yields information about the director distribution in a narrow layer rather than in the entire cell volume.

The method for describing the LC optical properties presented in this study can be applied to a variety of cells. The only significant limitation imposed on the LC system is the validity of geometrical optics approximation (the WKB method).

ACKNOWLEDGMENTS

This study was supported by St. Petersburg State University grants nos. 11.37.145.2014 and 11.37.161.2014 and (in part) by the Russian Foundation for Basic Research, project no. 15-03-09316 A.

APPENDIX

EXTINCTION COEFFICIENT IN A TWIST CELL WITH A LARGE HELIX PITCH

A homogeneous anisotropic medium is characterized by two extinction coefficients: $\sigma^{(o)}$ and $\sigma^{(e)}$. In the Born approximation [32, 35], they have the form

$$\sigma^{(i)} = \frac{k_0^4}{16\pi^2}\frac{e_\alpha^{(i)}e_\beta^{(i)}}{n^{(i)}\cos\delta^{(i)}} \times\sum_{s=o,e}\int d\Omega_{\mathbf{k}^{(s)}}\frac{n^{(s)}e_\mu^{(s)}e_\nu^{(s)}}{\cos^2\delta^{(s)}}G_{\alpha\mu\beta\nu}. \quad (A.1)$$

Here, the superscripts (i) and (s), which are related to the incident and scattered waves, respectively, take two values, corresponding to the (o) and (e) modes in a uniaxial medium. Here, $\delta^{(j)}$ are the angles between vectors $\mathbf{e}^{(j)}$ and $\hat{\varepsilon}\mathbf{e}^{(j)}$; $G_{\alpha\mu\beta\nu} = G_{\alpha\mu\beta\nu}(\mathbf{k}^{(s)} - \mathbf{k}^{(i)})$ is the Fourier transform of the correlation function of director fluctuations, $\hat{G}(\mathbf{r} - \mathbf{r}') = \langle\delta\hat{\varepsilon}(\mathbf{r})\delta\hat{\varepsilon}^*(\mathbf{r}')\rangle$ ($\delta\varepsilon_{\alpha\beta} = \varepsilon_a(n_\alpha\delta n_\beta + n_\beta\delta n_\alpha)$); and $n^{(j)}$ are the refractive indices of the ordinary and extraordinary waves, respectively,

$$G_{\alpha\mu\beta\nu}(\mathbf{q}) = \sum_{l=1}^{2}\langle|\delta n_l|^2\rangle(a_{l\alpha}a_{l\beta}n_\nu n_\mu + a_{l\alpha}a_{l\mu}n_\nu n_\beta + a_{l\nu}a_{l\mu}n_\alpha n_\beta + a_{l\nu}a_{l\beta}n_\alpha n_\mu), \quad (A.2)$$

where

$$\langle|\delta n_l|^2\rangle = \frac{k_B T\varepsilon_a^2}{K_{ll}q^2 + (K_{33} - K_{ll})(\mathbf{qn})^2} \quad (A.3)$$

is the mean square of fluctuations,

$$\mathbf{a}_2 = \frac{[\mathbf{q}\times\mathbf{n}]}{\sqrt{q^2 - (\mathbf{qn})^2}}, \quad (A.4)$$

$$\mathbf{a}_1 = [\mathbf{a}_2\times\mathbf{n}], \quad (A.5)$$

$\int d\Omega_{\mathbf{k}^{(s)}}$ denotes integration over all directions of unit vector $\mathbf{k}^{(s)}/k^{(s)}$.

In some cases, this expression can be significantly simplified and calculated analytically. At $q \to 0$, the correlation function of director fluctuations diverges as q^{-2}, which leads to a logarithmic divergence in integral (A.1). The q value may turn to zero only when the lengths of incident and scattered waves coincide. In this case, scattering of the $(o) \to (o)$ type is absent for geometrical reasons. Thus, a logarithmic divergence arises only in the case of $(e) \to (e)$ scattering. The contributions of the $(o) \to (e)$ and $(e) \to (o)$ scatterings to the extinction are reduced to single integrals in the form

$$\sigma_{(o,e)} = \tau_0\int_{-1}^{1} du\frac{1-u^2}{(1+au^2)^{3/2}} \times((1-u^2)(I_1(t_2) - I_1(t_1)) + I_2(t_2)), \quad (A.6)$$

$$\sigma_{(e,o)} = \frac{\tau_0 \sin^2\theta^*}{(1 + a\cos^2\theta^*)^{3/2}} \times \int_{-1}^{1} du(\rho_2^2 \sin^2\theta^*(I_1(t_2) - I_1(t_1)) + I_2(t_2)), \quad (A.7)$$

where θ^* is the angle between $n(r)$ and $k^{(i)}$,

$$\tau_0 = \frac{\omega^2 k_B T \varepsilon_a^2}{8\pi c^2 K_{33}\sqrt{\varepsilon_\perp \varepsilon_\parallel}}, \quad (A.8)$$

$$I_1(t) = \frac{t}{E(E + At + I_2^{-1}(t))}, \quad (A.9)$$

$$I_2(t) = (E^2 + 2tAE + t^2F^2)^{-1/2}, \quad (A.10)$$

$$E = (\rho_1 \cos\theta^* - u)^2, \quad (A.11)$$

$$A = \rho_1^2 \sin^2\theta^* + 1 - u^2, \quad (A.12)$$

$$F = \rho_1^2 \sin^2\theta^* + u^2 - 1, \quad (A.13)$$

$$\rho_1 = \sqrt{(1 + au)/(1 + a)}, \quad (A.14)$$

$$\rho_2 = \sqrt{(1 + a)/(1 + a\cos^2\theta^*)}, \quad (A.15)$$

$$a = \varepsilon_a/\varepsilon_\perp, \quad t_l = K_{ll}/K_{33}, \quad l = 1, 2.$$

The logarithmic contribution of the $(e) \to (e)$ scattering to the extinction can be written as

$$\sigma_{(e,e)}^{\ln} = \frac{\tau_0(\varepsilon_\perp\varepsilon_\parallel)^{3/2}\sin^2 2\theta^*}{P^2F_1}\frac{t_1(F_1 + F_2)}{(t_1F_2 + t_2F_1)}\ln\frac{L}{\lambda}, \quad (A.16)$$

where

$$P = \varepsilon_\parallel \cos^2\theta^* + \varepsilon_\perp \sin^2\theta^*, \quad (A.17)$$

$$F_l = (t_l^2\varepsilon_\parallel^2\cos^2\theta^* + t_l\varepsilon_\perp^2\sin^2\theta^*)^{1/2}. \quad (A.18)$$

Note that the logarithm of the L/λ ratio arises in this expression. The reason for this is that the director correlations are limited by the sample sizes. The contribution in the form (A.16) turns to zero at $\theta_* = 0$ and $\theta_* = \pi/2$. In fact, the contribution is nonzero for these angles. Therefore, along with the logarithmic contribution, the contribution linear in angle θ_* should be taken into account. To this end, we will calculate the extinction at $\theta_* = 0$ and $\theta_* = \pi/2$. The linear contribution can then be written as

$$\sigma_{(e,e)}^{\text{lin}} = \sigma_{(e,e)}(0) + \frac{2}{\pi}\theta_*\left(\sigma_{(e,e)}\left(\frac{\pi}{2}\right) - \sigma_{(e,e)}(0)\right). \quad (A.19)$$

Proceeding from the geometrical considerations, one can show that $\sigma_{(e,e)}(0) = \sigma_{(o,e)}(0)$. The $\sigma_{(e,e)}(\pi/2)$ value can be obtained numerically from expression (A.1). Thus, the extinction for an extraordinary ray takes the form

$$\sigma^{(e)} = \sigma_{(e,o)} + \sigma_{(e,e)}^{\ln} + \sigma_{(e,e)}^{\text{lin}}. \quad (A.20)$$

In a helicoidal medium with a large helix pitch, formula (A.1) retains meaning if one takes into account that $\mathbf{e}^{(j)}$, $n^{(j)}$, $\delta^{(j)}$, and $\hat{G}(\mathbf{q})$, which are functions of director $\mathbf{n}(z)$, depend on z. In fact expression (A.1) is used in the approximation of local homogeneity; i.e., the director in each layer is determined by angles θ_i and ϕ_i for this layer.

REFERENCES

1. Sh.-T. Wu and D.-K. Yang, *Fundamentals of Liquid Crystal Devices* (Wiley, New York, 2006).
2. W. Cai and V. Shalaev, *Optical Metamaterials* (Springer, New York, 2010).
3. J. Joannopoulos, R. Meade, J. Winn, and S. Johnson, *Photonic Crystals* (Princeton Univ. Press, Princeton, 2008).
4. K. Sakoda, Springer Ser. Opt. Sci. **80**, 1 (2001).
5. S. J. Woltman, G. D. Jay, and G. P. Crawford, Nat. Mater. **6**, 929 (2007).
6. V. Yu. Venediktov, G. E. Nevskaya, and M. G. Tomilin, Opt. Spectrosc. **111**, 113 (2011).
7. A. S. Matharu, S. Jeeva, and P. S. Ramanujam, Chem. Soc. Rev. **36**, 1868 (2007).
8. F. M. Leslie, Mol. Cryst. Liq. Cryst. **12**, 57 (1970).
9. D. W. Berreman and W. R. Heffner, J. Appl. Phys. **52**, 3032 (1981).
10. R. N. Thurston, J. Appl. Phys. **54**, 4966 (1983).
11. R. N. Thurston and D. W. Berreman, J. Appl. Phys. **52**, 508 (1981).
12. R. Hiring, W. Funk, H. R. Trebin, M. Shmidt, and H. Schmiedel, J. Appl. Phys. **70**, 4211 (1991).
13. H. Qi, T. X. Wu, and Sh.-T. Wu, Liq. Cryst. **30**, 367 (2003).
14. D. W. Berreman and T. J. Scheffer, Phys. Rev. A **5**, 1397 (1972).
15. D. W. Berreman, J. Opt. Soc. Am. **62**, 502 (1972); J. Opt. Soc. Am. **63**, 1374 (1973).
16. S. P. Palto, J. Exp. Theor. Phys. **92**, 552 (2001).
17. A. H. Gevorgyan, Phys. Rev. E **85**, 021704 (2012).
18. V. A. Belyakov and V. E. Dmitrienko, Sov. Phys. Solid State **15**, 1811 (1974).
19. V. E. Dmitrienko and V. A. Belyakov, Sov. Phys. Solid State **15**, 2213 (1974).
20. A. Lakhtakia and W. S. Weiglhofer, Microwave Opt. Technol. **12**, 245 (1996).
21. A. Yu. Val'kov, E. V. Aksenova, and V. P. Romanov, Phys. Rev. E **87**, 022508 (2013).
22. K. Rokushima and J. Yamakita, J. Opt. Soc. Am. **73**, 901 (1983).
23. F. Wang and A. Lakhtakia, Opt. Commun. **235**, 133 (2004).
24. M. Avendano-Alejo, Opt. Express **13**, 2549 (2005).
25. G. Panasyuk, J. Kelly, E. C. Gartland, and D. W. Allender, Phys. Rev. E **67**, 041702 (2003).

26. M. C. Mouguin, Bull. Soc. Franc. Miner. Cryst. **34**, 71 (1911).
27. V. S. Liberman and B. Ya. Zel'dovich, Phys. Rev. E **49**, 2389 (1994).
28. A. Yu. Savchenko and B. Ya. Zel'dovich, Phys. Rev. E **50**, 2287 (1994).
29. A. Yu. Val'kov, R. V. Grinin, and V. P. Romanov, Opt. Spectrosc. **83**, 221 (1997).
30. E. V. Aksenova, A. A. Karetnikov, A. P. Kovshik, V. P. Romanov, and A. Yu. Val'kov, Europhys. Lett. **69**, 68 (2005).
31. D. Langevin and M.-A. Bouchiat, J. Phys. **36**, 197 (1975).
32. A. Yu. Val'kov and V. P. Romanov, Sov. Phys. JETP **63**, 737 (1986).
33. J. Matheus and R. L. Walker, *Mathematical Methods of Physics* (Benjamin, New York, 1970).
34. E. V. Aksenova, B. B. Divinskii, A. A. Karetnikov, N. A. Karetnikov, A. P. Kovshik, E. V. Kryukov, and V. P. Romanov, J. Exp. Theor. Phys. **118**, 323 (2014).
35. A. Yu. Val'kov, V. P. Romanov, and A. N. Shalaginov, Phys. Usp. **37**, 139 (1994).

Translated by Yu. Sin'kov